Fluorinated Diphenylpolyenes: Crystal Structures and Emission Properties

Yoriko Sonoda,*,† Midori Goto,‡ Seiji Tsuzuki,§ and Nobuyuki Tamaoki†

Nanotechnology Research Institute and Technical Center, National Institute of Advanced Industrial Science and Technology (AIST), Higashi 1-1-1, Tsukuba, Ibaraki 305-8565, Japan, and Research Institute of Computational Sciences, National Institute of Advanced Industrial Science and Technology (AIST), Umezono 1-1, Tsukuba, Ibaraki 305-8568, Japan

Received: August 16, 2007; In Final Form: October 15, 2007

(*E*,*E*,*E*)-1,6-Diaryl(Ar)-1,3,5-hexatrienes (**2**, Ar = 4-fluorophenyl; **3**, Ar = 2,4-difluorophenyl; **4**, Ar = 2,4,6-trifluorophenyl; **5**, Ar = perfluorophenyl) and (*E*,*E*,*E*)-1-perfluorophenyl-6-phenyl-1,3,5-hexatriene (**6**) were prepared. The absorption and fluorescence spectra in methylcyclohexane solution showed only a small dependence on the fluorine ring substituent, and were similar to those of the unsubstituted parent compound (**1**, Ar = phenyl). The solid-state absorption and fluorescence spectra shifted to red relative to those in solution and strongly depended on the substituent. The emission from crystals **1**−**5** originated mainly from monomeric species with the maximum wavelength ($\lambda_{f(max)}$) of 440−465 nm, which overlapped the emission from molecular aggregates (**1**−**4**) or excimeric species (**5**) in the red region. Crystal **6** exhibited red-shifted ($\lambda_{f(max)}$ = 530 nm) and structureless emission due to excimers. The cocrystal of **1** and **5** (**1/5**) showed red-shifted ($\lambda_{f(max)}$ = 558 nm) and distinctly structured emission, not from exciplexes but from the excited states of molecular aggregates in which molecules **1** and **5** strongly interact already in the ground state. These assignments were confirmed by the results of fluorescence lifetime and quantum yield measurements in the solid state. Single-crystal X-ray structure analyses showed that the molecules were basically planar in each crystal, whereas the crystal packing was strongly substituent-dependent. Weak $\pi-\pi$ interactions in the herringbone (**1** and **2**) and in the π-stacked but largely offset structures (**3** and **4**) account for their predominantly monomeric origin of emission. The observation of excimer fluorescence from **5** was rather unexpected, since the molecules in this crystal were arranged in an offset stacking fashion due to perfluorophenyl−perfluorophenyl ($C_6F_5\cdots C_6F_5$) interaction. The structures of **6** and **1/5** considerably resembled each other, in which molecules were π-stacked with more face-to-face geometries than those in **5**, as a result of strongly attractive perfluorophenyl−phenyl ($C_6F_5\cdots C_6H_5$) interaction. Nevertheless, the fluorescence origin was clearly different for **6** and **1/5**. This can be ascribed to the difference in the strength of orbital−orbital interaction between molecular π-planes in the ground and excited states in crystals.

Introduction

Fluorescent organic solids are of great interest for photoactive materials due to their potential applications in light-emitting diodes (LEDs),[1−3] solid-state lasers,[4] and light-emitting electrochemical cells.[5] Up to now, a wide variety of compounds have been prepared in an effort to tailor the emission properties in the solid state.[6] They include distyrylbenzenes,[7−9] fluorenes,[10] and pyrenes.[11,12] Despite these extensive studies, however, our fundamental knowledge of solid-state fluorescence of organic molecules is rather limited and the understanding of the structure−property relationship is still insufficient.

Numerous examples of the structural studies of organic compounds show that the fluorination of aromatic rings often affords single crystals of quality suitable for X-ray analysis. In particular, intermolecular interaction between C_6F_5 and C_6H_5 rings is known to be strongly attractive.[13] Since the discovery of this interaction in the benzene−perfluorobenzene complex,[14] the interaction has been widely used in crystal engineering as a strong supramolecular synthon to steer face-to-face stacking geometry of aromatic molecules.[15−18] It is well-known that it can be utilized to prealign molecules for crystalline-state [2 + 2] photocycloaddition.[19−21] More recently, the interaction has been also proven to be effective for the formation of liquid crystals,[17b,22] hydrogels,[23] molecular glasses,[24] and even for the molecular aggregation on a graphite (HOPG) surface.[25] On the other hand, the nature of the forces in the interaction has also been studied both experimentally[26,27] and theoretically.[28,29] However, effects of the interaction between fluorinated rings, the $C_6F_5\cdots C_6H_5$ interaction in particular, on the fluorescence properties of organic crystals remain unknown.[30]

(*E*,*E*,*E*)-1,6-Diphenyl-1,3,5-hexatriene (DPH) (**1**, Chart 1) is a highly fluorescent molecule with a one-dimensional polyenic structure, and is commercially available as a fluorescence probe in biological membrane studies. The emission properties of DPH in solution have long attracted much attention because of its unique fluorescence behavior,[31] but its solid-state emission properties have yet to be clarified. We have recently reported that the emission wavelength was strongly dependent on the electron-donating/-withdrawing nature of the ring substituents.[32] Further, we have clarified that the crystals of a series of *p*-(*n*-alkoxy)-*p*′-nitro DPHs showed strong and red-shifted emission from monomeric species.[33] The crystal packing of these compounds depended on the length of the *n*-alkoxy chains, and

* Corresponding author. Fax: +81-29-861-4673. E-mail: y.sonoda@aist.go.jp.
† Nanotechnology Research Institute.
‡ Technical Center.
§ Research Institute of Computational Sciences.

10.1021/jp0766104 CCC: $37.00
Published on Web 12/06/2007

CHART 1

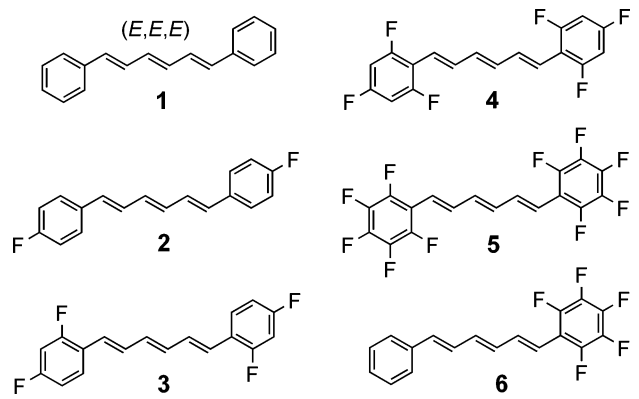

SCHEME 1

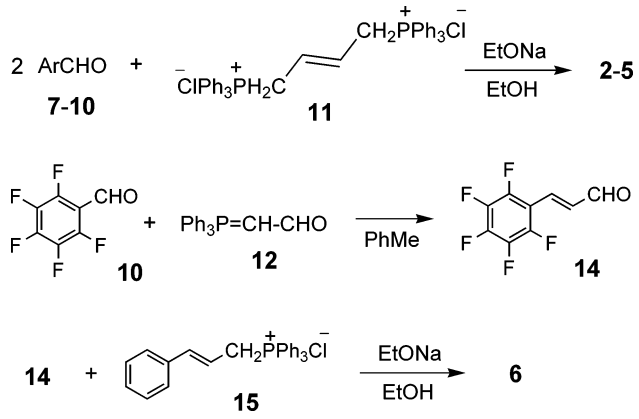

the difference in the packing (e.g., π-stacked vs herringbone) was clearly reflected in the emission wavelength.

The introduction of fluorine atoms into the different positions of the phenyl rings of DPH should change the type and strength of the intermolecular interactions, and should consequently change the molecular arrangements of the fluorophores in the crystals. Since the relative orientation of π-systems in three-dimensional space heavily affects the solid-state fluorescence properties of one-dimensional π-conjugated molecules such as DPH,[3] the investigation of the crystal structures and the solid-state emission properties of the fluorinated DPHs would contribute to our further understanding of the structure−property relationship for the solid-state fluorescence of organic molecules.

In this study, a series of ring-fluorinated DPHs (**2**−**6**, Chart 1) were synthesized. The solid-state absorption and fluorescence properties and the crystal structures of **1**−**6** and the cocrystal of **1** and **5** (**1**/**5**) were systematically investigated. The spectroscopic properties of **1**−**6** in solution were also studied for comparison.

Experimental Section

1. Materials. Compounds **2**−**6** were synthesized by the Wittig reaction (Scheme 1). Compound **1** (scintillation grade), 4-fluorobenzaldehyde (**7**), 2,4-difluorobenzaldehyde (**8**), 2,4,6-trifluorobenzaldehyde (**9**), perfluorobenzaldehyde (**10**), the bisphosphonium salt of (*E*)-1,4-dichloro-2-butene (**11**), (triphenylphosphoranylidene)acetaldehyde (**12**), and cinnamyl chloride (**13**) were purchased from Wako (**1** and **13**), TCI (**7**, **8**, **10** and **11**), Avocado (**9**), and Aldrich (**12**), and were used without further purification. Perfluorocinnamaldehyde (**14**) was prepared from **10** and **12** (Supporting Information). It should be noted that preparation of **14** from **10** and (1,3-dioxolan-2-yl)methyltriphenylphosphonium bromide was unsuccessful. Triphenylphosphonium salt **15** was prepared from **13**.[34] Pyrene (optical grade) was purchased from Fulka and used as received. All solvents used in the measurements of absorption and fluorescence spectra were of spectroscopic grade (Dojin).

2. Characterization. High-resolution mass spectra (MS) were obtained using a Hitachi M-80B instrument. IR spectra were recorded on a Mattson Infinity Gold FT-IR spectrometer. ^{1}H NMR spectra were recorded on a Varian Gemini-300 BB spectrometer (300.1 MHz) with tetramethylsilane (TMS) as internal reference. ^{19}F NMR spectra were recorded on a JEOL ECA-300 spectrometer (283 MHz), and were referenced to hexafluorobenzene (Aldrich, NMR grade) at 0.0 ppm. Purities of **1**−**6** were checked by HPLC.

3. (*E*,*E*,*E*)-1,6-Bis(4-fluorophenyl)-1,3,5-hexatriene (2). To a solution of **7** (2.12 g, 17.1 mmol) and **11** (5.46 g, 8.4 mmol) in ethanol (20 mL) was added a solution of sodium ethoxide in ethanol (0.60 M, 28 mL). The mixture was stirred under nitrogen atmosphere at room temperature for 45 h. Aqueous ethanol (60%, 100 mL) was added, and the mixture was stirred vigorously for 2 h. The resulting yellow precipitate was filtered off, washed with water (20 mL), and dried. The crude product was an *E*−*Z* isomeric mixture of **2**. The mixture was dissolved in toluene (80 mL), and the solution was refluxed for 4−5 h with a trace amount of iodine to induce *Z*-to-*E* thermal isomerization. After evaporating the solvent, the resulting pale yellow solid **2** was recrystallized twice from toluene. Yield 10−20%. mp 188−190 °C (lit.[35] 188−190 °C); MS Found: M^+, 268.1052. Calcd for $C_{18}H_{14}F_2$: M, 268.1062; ν_{max} (KBr) 1587, 1508, 1418, 1239, 1159, 1095, 995, 923, 866, 823, and 788 cm^{-1}; ^{1}H NMR ($CDCl_3$) δ 7.35−7.40 (4H, m, arom), 6.98−7.04 (4H, m, arom), 6.79 (2H, apparently (app) ddd, J = 15.3, 6.9, and 2.9, triene), 6.55 (2H, app d, J = 15.5, triene), 6.49 (2H, app dd, J = 7.0 and 3.0, triene); ^{19}F NMR ($CDCl_3$) δ 47.6−47.7 (2F, m); UV−vis λ_{max} (MeCN) 349 nm (ϵ = 75 700). Single crystals of **2** for X-ray analysis were obtained by very slow evaporation of toluene solvent at room temperature in the dark.

4. (*E*,*E*,*E*)-1,6-Bis(2,4-difluorophenyl)-1,3,5-hexatriene (3). Triene **3** was prepared from **8** and **11** by a procedure similar to that for **2**. Recrystallization from toluene gave yellow needles, which were suitable for single-crystal X-ray analysis. Yield 65%. mp 164−165 °C; MS Found: M^+, 304.0874. Calcd for $C_{18}H_{12}F_4$: M, 304.0874; ν_{max} (KBr) 1585, 1491, 1429, 1263, 1133, 1088, 1000, 961, 849, and 810 cm^{-1}; ^{1}H NMR ($CDCl_3$) δ 7.42−7.50 (2H, m, arom), 6.76−6.92 (6H, m, arom and triene), 6.67 (2H, app d, J = 15.7, triene), 6.53 (2H, app dd, J = 7.0 and 3.0, triene); ^{19}F NMR ($CDCl_3$) δ 51.0−51.1 (2F, m), 48.1−48.2 (2F, m); UV−vis λ_{max} (MeCN) 349 nm (ϵ = 68 900).

5. (*E*,*E*,*E*)-1,6-Bis(2,4,6-trifluorophenyl)-1,3,5-hexatriene (4). Triene **4** was prepared from **9** and **11** by a procedure similar to that for **2**. The reaction temperature was 45 °C. Recrystallization from toluene gave yellow crystals, which were suitable for X-ray analysis. Yield 91%. mp 178−182 °C (sublimation); MS Found: M^+, 340.0687. Calcd for $C_{18}H_{10}F_6$: M, 340.0686; ν_{max} (KBr) 1591, 1486, 1440, 1170, 1114, 1020, 997, and 844 cm^{-1}; ^{1}H NMR ($CDCl_3$) δ 7.11 (2H, app ddd, J = 16.0, 7.1, and 2.9, triene), 6.62−6.72 (4H, m, arom), 6.55 (2H, app d, J = 15.8, triene), 6.52 (2H, app dd, J = 6.4 and 3.6, triene); ^{19}F NMR ($CDCl_3$) δ 52.4−52.5 (2F, m), 52.1 (4F, m); UV−vis λ_{max} (MeCN) 345 nm (ϵ = 74 200).

6. (*E*,*E*,*E*)-1,6-Bis(perfluorophenyl)-1,3,5-hexatriene (5). Triene **5** was prepared from **10** and **11** by a procedure similar

to that for **2**. Recrystallization from toluene gave yellow solid. Yield 82%. mp 166−168 °C (sublimation); MS Found: M^+, 412.0290. Calcd for $C_{18}H_6F_{10}$: M, 412.0308; ν_{max} (KBr) 1649, 1608, 1526, 1496, 1418, 1365, 1211, 1164, 1122, 1003, and 956 cm^{-1}; ^1H NMR ($CDCl_3$) δ 7.18 (2H, app ddd, J = 16.0, 7.1, and 2.7, triene), 6.59 (2H, app dd, J = 6.6 and 3.5, triene), 6.56 (2H, app d, J = 15.8, triene); ^{19}F NMR ($CDCl_3$) δ 19.2−19.3 (4F, m), 5.8−6.0 (2F, m), (−1.2)−(−1.0) (4F, m); UV−vis λ_{max} (MeCN) 346 nm (ϵ = 74 300). Single crystals of **5** for X-ray analysis were obtained by very slow evaporation of acetonitrile solvent at room temperature in the dark.

7. (*E*,*E*,*E*)-1-Perfluorophenyl-6-phenyl-1,3,5-hexatriene (6). To a solution of **14** (1.00 g, 4.5 mmol) and **15** (1.87 g, 4.5 mmol) in ethanol (22 mL) was added a solution of sodium ethoxide in ethanol (0.30 M, 15 mL). The mixture was stirred under nitrogen atmosphere at room temperature for 25 h. The resulting pale yellow precipitate was filtered off, washed with water (60 mL), and dried. Recrystallization of the crude product (predominantly *E*,*E*,*E*) from toluene gave yellow thin plates, which were suitable for X-ray analysis. Yield 47%. mp 159−160 °C (sublimation); MS Found: M^+, 322.0748. Calcd for $C_{18}H_{11}F_5$: M, 322.0780; ν_{max} (KBr) 1583, 1523, 1495, 1354, 988, 956, 855, 749, and 691 cm^{-1}; ^1H NMR ($CDCl_3$) δ 7.25−7.45 (5H, m, arom), 7.18 (1H, dd, J = 16.1 and 10.7, triene), 6.89 (1H, dd, J = 15.4 and 10.4, triene), 6.67 (1H, d, J = 15.5, triene), 6.62 (1H, dd, J = 15.0 and 10.4, triene), 6.47 (1H, d, J = 16.0, triene), 6.45−6.53 (1H, m, triene); ^{19}F NMR ($CDCl_3$) δ 18.8−18.9 (2F, m), 4.7−4.9 (1F, m), (−1.5)−(−1.3) (2F, m); UV−vis λ_{max} (MeCN) 351 nm (ϵ = 72 900).

8. Cocrystal of 1 and 5 (1/5). Trienes **1** (0.058 g, 0.25 mmol) and **5** (0.103 g, 0.25 mmol) were dissolved in acetonitrile (100 mL). Cocrystal **1/5** suitable for X-ray analysis was obtained by very slow evaporation of the solvent at room temperature in the dark. mp 169−170 °C; ν_{max} (KBr) 1522, 1497, 1449, 1418, 1357, 1300, 1204, 1074, 991, 955, 752, and 692 cm^{-1}.

9. Measurements of Absorption Spectra. Absorption spectra in solution were measured in air at room temperature using a Shimadzu UV-3150 spectrometer. All solutions were highly diluted ((1−2) × 10^{-5} M). Absorption spectra in the solid state were obtained by Kubelka−Munk conversion of diffuse reflectance spectra. The reflectance spectra were recorded on a Jasco V-560 spectrometer equipped with an integrating sphere accessory (Model ISV-469), using a fluorescence cut filter (HOYA, U-330). The sample solids were placed between quartz plates (40 × 10 mm^2).

10. Measurements of Fluorescence Spectra, Fluorescence Quantum Yields, and Fluorescence Lifetimes. The corrected fluorescence and excitation spectra for the solutions of **1**−**6** and those for the crystals of **1**−**6** and **1/5** were measured in air at room temperature using a SPEX Fluorolog-3 spectrometer. For the fluorescence measurements in solution, the excitation wavelength (λ_{ex}) was set at 350 nm. Concentration of the sample solutions was (1.0−1.5) × 10^{-6} M. Fluorescence quantum yields (ϕ_f) of **1**−**6** in solution were determined using a solution of quinine sulfate in 1 N H_2SO_4 as a standard (ϕ_f = 0.546).[36] Fluorescence spectra of the crystalline samples were recorded using the front face geometry. The sample crystals were placed between quartz plates (40 × 10 mm^2) on the sample holder. For **1**−**5** and **1/5**, λ_{ex} was set at 360 nm, and for **6**, λ_{ex} was set at 390 nm. Values of ϕ_f in the solid state were estimated by comparison of fluorescence peak areas for the thick crystalline samples of **1**−**6** and **1/5** with that for pyrene (ϕ_f = 0.64 at 293 K).[37] Fluorescence decay curves in solution and in the solid state were obtained by the time-correlated single-photon-counting (TCSPC) method, using a HORIBA NAES 700 equipped with a subnanosecond nitrogen laser system (λ_{ex} = 337 nm). The monitor wavelength (λ_{mon}) was set at 450 nm in all solution experiments. In the solid-state measurements, λ_{mon} was set at the wavelengths indicated in Table 3.

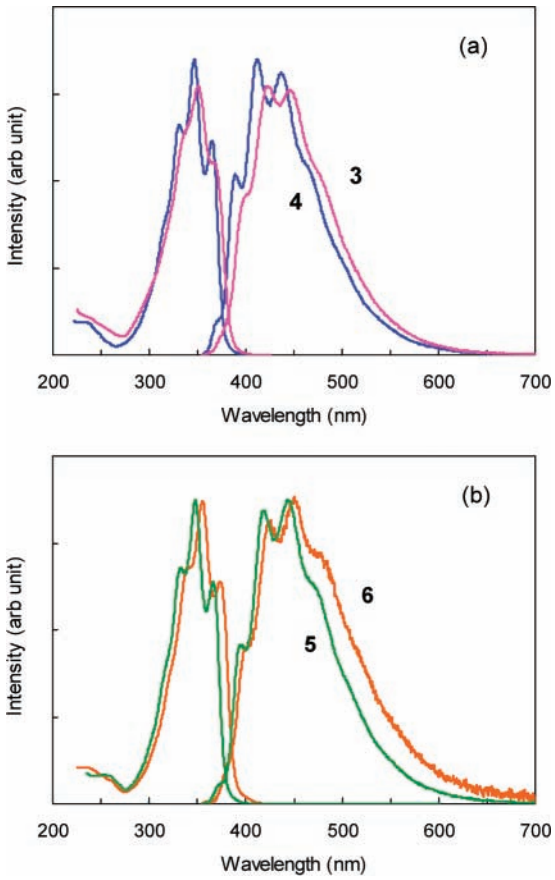

Figure 1. Absorption and fluorescence spectra of (a) **3** and **4** and (b) **5** and **6** in methylcyclohexane.

It should be noted that solid-state fluorescence measurements (of crystalline materials) can be difficult as the morphology of the crystals can be an issue. In the current study, the samples were not ground to a powder.

11. Single-Crystal X-ray Structure Analyses. The single-crystal X-ray diffraction measurements of **2**−**6** and **1/5** were performed at 183 K using a CCD area-detector diffractometer with graphite monochromated Mo Kα radiation (λ = 0.710 73 Å). Data collection, reduction, and empirical absorption correction were carried out using SMART,[38] SAINTPLUS,[38] and SADABS (2001).[38] The structure was solved by direct methods using SIR92[39] and refined by full matrix least-squares on F^2 with SHELXTL.[40] The non-hydrogen atoms were refined anisotropically. Hydrogen atoms were placed in geometrically calculated positions and refined by a riding model.

12. Computational Method. The Gaussian 03 program[41] was used for the ab initio molecular orbital calculations. All ground-state geometries were optimized at the HF/6-31G* level. C_{2h} symmetry was assumed for **1**−**5**, and C_s symmetry was assumed for **6**. The 6-311G** basis set was used for CIS[42] and TD-B3LYP[43] calculations.

Results and Discussion

1. Absorption and Fluorescence Properties in Solution. The absorption and fluorescence spectra of **1**−**6** in methylcyclohexane (MCH) are shown in Figures 1 and S1, and

TABLE 1: Absorption and Fluorescence Data of 1−6 in Methylcyclohexane[a]

compd	λ_a (nm)	λ_f (nm)	ϕ_f	τ_s (ns)
1	338, 353, 372	377, 399, 423, 449, 476	0.38	7.1
2	337, 351, 369	375, 397, 421, 447, 473	0.40	7.4
3	337, 351, 367	399, 423, 447, 477	0.47	6.8
4	332, 347, 365	369, 389, 412, 437, 464	0.57	6.2
5	333, 348, 367	372, 395, 419, 444, 470	0.43	8.0
6	340, 356, 374	380, 402, 424, 451, 482	0.059	0.59 (97%) 5.0 (3%)

[a] Underlined values are the wavelengths of $\lambda_{a(max)}$ and $\lambda_{f(max)}$.

summarized in Table 1. The spectra of **1** and **2** (Figure S1) agreed with those reported.[35,44]

1.1. Absorption Properties. The introduction of fluorine atoms into the phenyl rings of DPH induced only a small change in the absorption wavelength (λ_a), probably a result of a combination of the induction and electron back-donation effects of the fluorine atoms.[45] This indicates that λ_a values of these compounds are almost independent of the fluorine substituent when the molecules are isolated. A similar result has been reported for fluorinated distyrylbenzenes.[45] It should be added that the absorption spectrum of an equimolar mixture of **1** and **5** in MCH was exactly the same as the sum of the spectra of the individual molecules, indicating no formation of the molecular complex of **1** and **5** in solution in the concentration range examined.

The absorption spectra showed clear vibrational structures due to vibronic coupling. The energy spacings were 1200−1500 cm^{-1}, corresponding to the C=C and C−C stretches of conjugated trienes.[46] Exceptionally, the spectrum of **3** was only weakly structured. This may arise from the fact that the difference between the molecular geometries in the ground and excited states of **3** differs significantly from those of the other compounds.[47]

1.2. Fluorescence Properties. 1.2.1. Fluorescence Spectra. The fluorescence spectra also showed minimal changes upon fluorine substitution (Figures 1 and S1). The fluorescence wavelengths (λ_f) for the isolated molecules of these compounds were not largely affected by substituents, as in the case of λ_a (Table 1). The fluorescence spectra of **1**−**6** showed vibrational structures with the spacings of 1250−1450 cm^{-1}, although the spectrum of **3** was again less structured.

Since all spectra were measured under highly diluted conditions, only monomeric species should be involved in the absorption and emission processes. However, the observed overlaps of the absorption and emission spectra were rather small, and no mirror-image relationship was seen between them (Figures 1 and S1). For **1** and **2**, such an anomalous spectral behavior has been understood in terms of dual fluorescence from the two lowest excited singlet states, S_1 and S_2.[31,35] Since the peak positions and spectral shapes of the absorption and emission spectra of **3**−**6** were all similar to those of **1** and **2**, it is very probable that **3**−**6** also exhibit S_1/S_2 dual fluorescence at least in this solvent.

Although the positions of λ_f for **6** in MCH were not greatly different from those for **1**−**5**, its emission intensity in the red region clearly increased relative to those of the symmetrically substituted compounds (Figure 1b). This red-shifted emission of **6** would originate from a charge-transfer excited state (CT*), formed by intramolecular CT from an initially photoproduced, locally excited state (LE*). The CT character of this state is evidenced by the fact that the fluorescence intensity in the red region increased as the solvent polarity increased (Figure S2). Values of ϕ_f were small in polar solvents, probably due to the forbidden nature of the CT* emission.[47] Solvent effects on the absorption spectra were small. Thus, the emission of **6** in MCH is mainly from LE*, with which the red-shifted emission from CT* is overlapped as a minor component.

The excitation energies of S_0-S_1 and S_0-S_2 transitions were calculated using TD-DFT(B3LYP) and CIS methods. The results are summarized in Tables S1 and S2. Both calculations show that the excitation energies of these transitions are not greatly different for all compounds studied. This is in accordance with the observed small substituent dependence of λ_a and λ_f of **1**−**6** in solution.

1.2.2. Fluorescence Quantum Yields and Lifetimes. Table 1 summarizes ϕ_f and fluorescence lifetimes (τ_s) of **1**−**6** in MCH.[48] The values of ϕ_f for **1**−**5** were moderate, whereas ϕ_f for **6** was relatively small. This can be attributed to much greater efficiency of *Z*−*E* photoisomerization for **6** than those for **1**−**5** in this solvent, as shown by the absorption spectral changes before and after ϕ_f measurements.[49] Repeated measurements of the fluorescence spectrum of **6** caused a considerable decrease in its emission intensity. However, no change was observed in its spectral shape or peak position, suggesting that the photoproduced *Z* isomer(s) is nonfluorescent or much less fluorescent than its parent *E*,*E*,*E* isomer.

Fluorescence decay curves of **1**−**5** were able to be analyzed by a single-exponential function to give τ_s values ranging from 6 to 8 ns. In contrast, the decay curve of **6** could be fitted only by a biexponential function, in agreement with the observation of the dual fluorescence from LE* and CT*. The dependence of τ_s on λ_{mon} reveals that $\tau_s = 0.59$ and 5.0 ns are due to the LE* fluorescence and CT* fluorescence, respectively. Thus the τ_s value of the LE* state in **6** is much shorter than the τ_s values measured for **1**−**5**, which presumably correspond to the decay of their LE* states. It should be noted, however, that the radiative rate constant ($k_f = \phi_f/\tau_s$) for the LE* emission of **6** is expected to be on the same order of magnitude as the values for the LE* emission of **1**−**5**, because of the much smaller ϕ_f of **6** than those of **1**−**5**. Although asymmetric **6** exhibited CT* emission even in low-polar MCH, the relatively long τ_s, probably a very small ϕ_f, and the resulting small k_f suggest the forbidden character of the transition.

2. Absorption and Fluorescence Properties in the Solid State. The absorption and fluorescence spectra for the crystals of **1**−**6** and **1/5** are shown in Figure 2 and summarized in Table 2.

2.1. Absorption Properties. The absorption spectra in the solid state showed main (M) bands, whose absorption maxima ($\lambda_{a(max)}$) were located in the region of 380−390 nm for all compounds studied. The substituent dependence of $\lambda_{a(max)}$ of the M band was small as that of $\lambda_{a(max)}$ in solution. The positions of $\lambda_{a(max)}$ for the M bands shifted to red from those in MCH by 30−40 nm (Tables 1 and 2). The difference between $\lambda_{a(max)}$ in solution and that of the M band in the solid state was thus relatively small. These strongly suggest that the M band is the absorption of monomeric species in the solid state. The M bands in **1**−**4** showed some vibrational structures. Although the structures

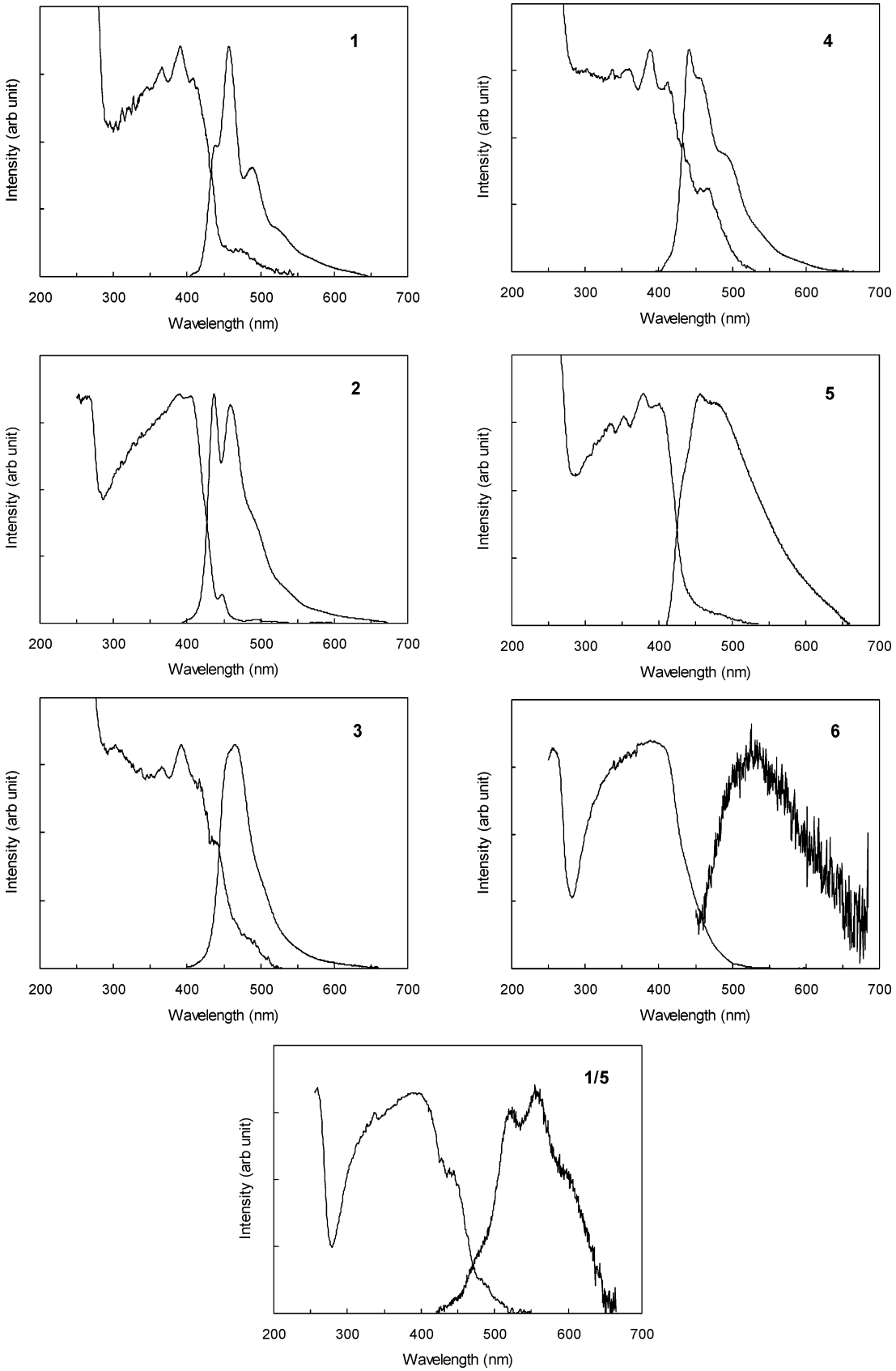

Figure 2. Absorption and fluorescence spectra of crystals **1**−**6** and cocrystal **1/5**.

were weaker than in solution, the spacings of 1000−2000 cm^{-1} in the solid state are similar to the values in MCH.

For the crystals other than **6**, red-shifted (R) absorption bands were additionally observed. The intensity of the R band was strongly dependent on the substituent. The R bands were only weakly seen in the spectra of **1** and **2**, while in **3** and **4**, they were much more strongly observed. Thus the R band intensity increased as the aromatic ring was more fluorinated, from **1** to **4**. However, the R band in **5** became much smaller than in **4**, and in the case of **6**, the band was not clearly observed. On the

TABLE 2: Absorption and Fluorescence Data for the Crystals of 1−6 and 1/5[a]

	λ_a (nm)			
compd	B[b]	M	R	λ_f (nm)
1	276	366, 391, 409	478	438, 457, 488, 524
2	265	390, 405	448, 494	437, 459, 491, 539
3	260	365, 392, 417	440, 488	456, 465, 503
4	258	360, 388, 412	435, 467	441, 457, 491, 538, 590
5	258	334, 353, 379, 400	484	431, 457, 483
6	259	388	(none)	530
1/5	260	362, 393	445, 480	439, 472, 523, 558, 604

[a] Underlined values are the wavelengths of $\lambda_{a(max)}$ and $\lambda_{f(max)}$. [b] Absorption due to benzene rings.

other hand, a strong R band was observed in the spectrum of cocrystal **1/5** in the wavelength region longer than approximately 420 nm. The spectrum of **1/5** differed clearly from those of its individual components, **1** and **5**, in which the R bands were only weakly seen. These strongly suggest that the R band reflects the strength of intermolecular interactions in the crystals. It is very probable that the R band is the absorption of molecular aggregates in the solid state.

The solid-state absorption spectrum was thus strongly dependent on the substituent, in contrast to the spectrum in solution.

2.2. Fluorescence Properties. 2.2.1. Fluorescence Spectra. The solid-state fluorescence spectrum was also strongly substituent-dependent. The spectra of **1**−**4** showed the fluorescence peak maxima ($\lambda_{f(max)}$) in the range of 440−465 nm (Table 2). The spectra of **1**, **2**, and **4** were clearly structured, although **3** was again exceptional as in solution. The spacings of 1000−2000 cm^{-1} were similar to the values in the M absorption bands. The fluorescence spectra were largely overlapped with the M absorption bands, resulting in the relatively small Stokes shifts of 1500−2000 cm^{-1}, calculated from the longest λ_a of the M band and the shortest λ_f. These indicate that the emission of **1**−**4** is originated mainly from the monomeric species in the solid state. On the other hand, the emission from molecular aggregates that corresponded to the red-shifted R absorption band was overlapped with the monomer emission in the relatively red region, as suggested by the λ_{ex} dependence of the fluorescence spectrum and by the emission-wavelength (λ_{em}) dependence of the fluorescence excitation spectrum.

The fluorescence spectrum of **5** in the shorter wavelength region was weakly structured and largely overlapped with the M absorption band, suggesting its monomeric origin of emission. The positions of λ_f were similar to those in the other symmetrically substituted **1**−**4** (Table 2). In the red region, the emission intensity clearly increased relative to those in **1**−**4**. The spectrum was broad and structureless in this region. In view of the fact that the R absorption band was only weakly observed, the red-shifted emission probably originates from excimeric species. Thus, the solid-state emission from **5** is considered to be the overlap of the monomer and excimer fluorescence.

By contrast, the spectrum of **6** was broad and structureless in all the spectral range. The position of $\lambda_{f(max)}$ was largely red-shifted to 530 nm. The overlap of the absorption and emission spectra was small, with the large Stokes shift of 6905 cm^{-1}. Combined with the absence of the R absorption band, these spectral features in the emission clearly show that crystal **6** exhibits excimer fluorescence. Consistently, the fluorescence spectrum showed no λ_{ex} dependence, and the fluorescence excitation spectrum was fundamentally the same as its absorption spectrum.

Cocrystal **1/5** showed a spectrum entirely different from those of **1** and **5**; $\lambda_{f(max)}$ was observed at 558 nm, strongly red-shifted from $\lambda_{f(max)}$ of **1** and **5** by 101 nm. The spectrum was distinctly

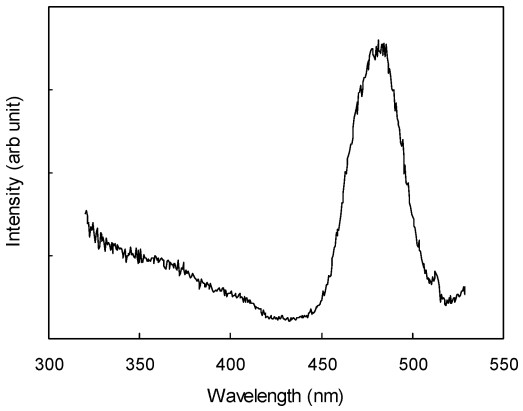

Figure 3. Fluorescence excitation spectrum of cocrystal **1/5**.

structured with the spacings of 1199 and 1365 cm^{-1}. A combination of the large red shift and clear vibrational structures in the fluorescence spectrum and the strong R band in the absorption spectrum indicates that the emission of **1/5** is originated not from exciplexes, which have repulsive potentials in the ground state, but from the excited states of molecular aggregates in which molecules **1** and **5** strongly interact already in the ground state. Red-shifted and structured fluorescence due to molecular aggregates has also been observed for the thin film of *p*,*p*′-dimethoxy-substituted DPH[32] and the nanoparticles of phenylenevinylene oligomer.[7] In accordance with the above assignment, the excitation spectrum obtained at $\lambda_{em} = 558$ nm showed the peak with the maximum at 482 nm, as shown in Figure 3. This peak should correspond to the R band at 480 nm in the absorption spectrum. The peaks at 362 and 393 nm, which are λ_a of the M absorption band, were only very weakly observed in the excitation spectrum, indicating that the monomeric species of **1** and **5** are not responsible for the emission at 558 nm. Also, the excitation spectrum obtained at $\lambda_{em} = 439$ nm showed the peak with the maximum of 362 nm, which suggests that the weak emission at 439 nm is of monomeric origin.

2.2.2. Fluorescence Lifetimes and Quantum Yields. Table 3 summarizes τ_s data for the crystals of **1**−**6** and **1/5**. In contrast to the cases in solution, the fluorescence decay curves in the solid state could be fitted only by a biexponential function for all the compounds studied. A complex decay behavior is typical for organic solids, and can be attributed to the efficient migration of excitation energy in the solid state. Also, it could be attributed to quenching by site defects.

The λ_{mon} dependence of τ_s for **1**−**4** shows that $\tau_s = 1-2$ ns and $\tau_s = 5-7$ ns (or longer) are respectively due to the emission from monomer and molecular aggregates of these compounds. The values around $\tau_s = 1$ ns are typical for the monomeric emission from small organic dye molecules in the solid state.[3]

The excimer fluorescence in the solid state often shows bi- or multiexponential decay behavior, which may be a result of

TABLE 3: Fluorescence Lifetimes for the Crystals of 1−6 and 1/5

compd	λ_{mon} (nm)	τ_s (ns)		χ^2
1	438	1.0 (91%)	5.4 (9%)	1.08
	457	1.0 (90%)	5.1 (10%)	1.21
	488	1.1 (79%)	4.9 (21%)	1.37
	524	1.7 (65%)	5.6 (35%)	1.31
	570	1.9 (45%)	5.3 (55%)	2.06
2	459	0.90 (95%)	5.6 (5%)	1.15
3	465	0.88 (86%)	6.3 (14%)	1.63
4	440	0.85 (97%)	9.4 (3%)	1.53
	457	0.86 (87%)	7.3 (13%)	1.46
	490	1.0 (90%)	7.2 (10%)	1.33
	538	1.0 (76%)	5.6 (24%)	1.20
5	457	1.1 (93%)	6.5 (7%)	1.23
6	530	0.96 (82%)	5.4 (18%)	1.29
1/5	472	1.1 (88%)	6.9 (12%)	1.56
	523	2.8 (86%)	8.5 (14%)	1.31
	558	2.9 (87%)	7.1 (13%)	1.32
	604	3.0 (87%)	9.7 (13%)	1.31
	630	2.5 (79%)	5.7 (21%)	1.59

CHART 2

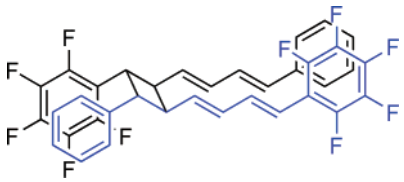

complex kinetics that include different types of excimers and other aggregated complexes in the excited state.[50] The biexponential decay behavior for **5** and **6** is therefore consistent with the excimer formation in these crystals. The two components of τ_s have also been reported for the excimers of 2,7-fluorenevinylene-based trimers in spin-coated film samples.[51]

The fluorescence decay behavior of cocrystal **1/5** seemed to be much more complex than those for the other single-component crystals. Although biexponential fitting is probably not perfect in this case, $\tau_s = 1.1$ ns obtained at $\lambda_{mon} = 472$ nm and the longer τ_s at longer λ_{mon} are assignable to the emission from monomer and molecular aggregates, respectively.

Although ϕ_f values for organic solids are difficult to determine precisely due to the intrinsic inhomogeniety of solid samples, ϕ_f values for crystals **1**−**6** and **1/5** were roughly estimated using pyrene as a standard. The obtained values of $\phi_f = 0.1-0.2$ for **1**[32] and $\phi_f = 0.05-0.1$ for **2**−**5** were moderate compared as organic solids, while $\phi_f = 0.005$ or below for **6** and $\phi_f = 0.01-0.02$ for **1/5** were considerably lower. Such small ϕ_f values for **6** and **1/5** are indicative of the efficient radiationless processes from the excimers and molecular aggregates. Indeed, they underwent intermolecular [2 + 2] photocycloaddition in the solid state as described below.

3. Solid-State Photoreactivity. Compounds **1**−**4** were photostable whereas **5**, **6**, and **1/5** were photoreactive in the crystalline state. The order of reactivity was **6** > **1/5** ≫ **5**. In each case, the main photoproduct was shown by NMR, MS, and UV−vis spectroscopic analyses to be a face-to-face dimer formed by [2 + 2] cycloaddition of the terminal double bonds of the trienes. The chemical structure of the photodimer of **6** is shown in Chart 2. Prolonged irradiation of **5**, **6**, and **1/5** induced [2 + 2] polymerization to yield higher molecular weight products. Details of the photopolymerization will be reported elsewhere. However, it should be noted here that all spectra were measured with minimum exposure to light in the present study.

The [2 + 2] photocycloaddition of olefins in single-component crystals is in general considered to proceed via excimers.[19] Therefore, the observation of photocycloaddition in **5** and **6** strongly supports the formation of excimer in these crystals.

4. Crystal Structures. Table 4 shows the single-crystal data of **1**−**6** and **1/5** obtained by X-ray structure analyses. The ORTEP representations of the molecular structures are displayed in the Supporting Information.

4.1. Molecular Structures. Molecules in each crystal were basically planar, although the planarity of **2** was somewhat lower probably due to the packing reason. The mean deviations from the least-squares plane defined by the DPH moiety and the torsion angles around the Ar−CH single bonds in the crystals are summarized in Table S3.

4.2. Crystal Packing. Figure 4 shows the crystal packing diagrams for **2**−**6** and **1/5**. Crystals **1** and **2** had herringbone structures. The dihedral angles for the DPH planes of the nearest molecules were 75.6(1)° for **1**[52] and 53.2(1)° for **2**. By contrast, crystals **3**−**6** and **1/5** had π-stacked structures.[54] Table 5 and Chart 3 summarize the relative positions of the DPH π-planes of the neighboring two molecules in the stacks. The large d and small θ in **3** and **4** suggest that the stacking interactions between the aromatic rings are rather weak in these crystals. More fluorination of the rings decreased the d value considerably. In **5**, d was reduced to 4.9 Å as a result of $C_6F_5\cdots C_6F_5$ interaction, although $\theta = 34°$ was still much smaller than 90°. This results in the largely offset stacking structure of **5**. The offset structure has also been observed for a derivative of *s-cis E,E*-1,4-di(perfluorophenyl)-1,3-butadiene.[57] The structures of **6** and **1/5** considerably resembled each other, in which molecules were packed in a nearly face-to-face stacking fashion.[58] The value d considerably decreased to 3.7−3.8 Å and θ greatly increased to 58−63° from the corresponding values in **5**. The proximity of the stacking molecules clearly arises from the strongly attractive $C_6F_5\cdots C_6H_5$ intermolecular interaction in crystals **6** and **1/5**. The experimental observation that the offset of **5** was larger than those of **6** and **1/5** is consistent with the theoretical prediction that $C_6F_6\cdots C_6F_6$ interaction energy is smaller than that of $C_6F_6\cdots C_6H_6$ for the two aromatic rings arranged in a face-to-face geometry.[29]

5. Relationship between the Solid-State Spectroscopic Properties and the Crystal Structure. *5.1. Absorption Properties.* The position of $\lambda_{a(max)}$ of the M absorption bands in the solid state was shifted to red by 30−40 nm from those in MCH solution for all compounds studied. This red shift would be mainly due to the planarization of the molecule in the solid state. In solution, the Ar−CH single bonds rotate almost freely. Ab initio calculations show that the torsional potentials for these bonds are very shallow and that an about 15°-twisted structure is the most stable.[59] However, in the solid state, the rotation is restricted and the molecules have basically planar conformation as shown by the crystal structure analysis. The resulting more effective conjugation leads to the red shifts of $\lambda_{a(max)}$ in the solid-state spectra. The small substituent dependence of $\lambda_{a(max)}$ of the M absorption band is a result of a combination of the facts that λ_a values for the isolated molecules are all similar, and that the molecular planarity is not greatly different in each crystal.

In sharp contrast, the intensity of the R absorption band was strongly dependent on the substituent. This would come from the difference in the strength of the orbital−orbital interaction between DPH π-planes in each crystal. Clearly, weak $\pi-\pi$ interactions in the herringbone structures result in the weak R bands in the absorption spectra of **1** and **2**. The increase in the

TABLE 4: Crystal Data of 1−6 and 1/5

	1[a]	2	3	4	5	6	1/5
formula	$C_{18}H_{16}$	$C_{18}H_{14}F_2$	$C_{18}H_{12}F_4$	$C_{18}H_{10}F_6$	$C_{18}H_6F_{10}$	$C_{18}H_{11}F_5$	$C_{36}H_{22}F_{10}$
formula weight	232.32	268.29	304.28	340.26	412.23	322.27	644.54
crystal color; habit	colorless	pale yellow; needle	yellow; rectangular	yellow; rectangular	yellow; plate	yellow; plate	yellow; plate
crystal size (mm)	0.15 × 0.25 × 0.35	0.20 × 0.04 × 0.03	0.30 × 0.10 × 0.10	0.30 × 0.20 × 0.20	0.30 × 0.10 × 0.05	0.30 × 0.30 × 0.02	0.30 × 0.30 × 0.02
crystal system	orthorhombic	triclinic	triclinic	triclinic	triclinic	triclinic	triclinic
space group	*Pbca*	$P\bar{1}$	$P\bar{1}$	$P\bar{1}$	$P\bar{1}$	$P\bar{1}$	$P\bar{1}$
a (Å)	7.730(2)	9.582(4)	6.752(3)	6.9822(8)	5.939(1)	6.091(2)	6.062(1)
b (Å)	9.881(2)	11.523(5)	7.414(3)	7.2167(9)	8.102(2)	8.179(3)	8.220(2)
c (Å)	18.096(3)	12.890(5)	7.515(3)	7.3338(9)	8.559(2)	14.720(5)	14.480(3)
α (deg)	90	85.425(8)	85.677(8)	88.901(2)	80.335(3)	78.667(5)	85.410(4)
β (deg)	90	84.296(9)	73.170(8)	79.877(2)	78.540(4)	87.639(5)	89.540(4)
γ (deg)	90	75.810(8)	79.341(7)	77.540(2)	73.542(4)	83.470(6)	83.890(4)
V (Å^3)	1382.175	1370.8(10)	353.8(3)	355.15(7)	384.4(2)	714.3(4)	715.1(3)
Z	4	4	1	1	1	2	1
D_{calc} (g/cm^3)	1.12	1.300	1.428	1.591	1.781	1.498	1.497
T (°C)	20	−90	−90	−90	−90	−90	−90
mp (°C)	196[b]	190	165	182	168	160	170
R_1 ($I > 2\sigma(I)$)	0.039[c]	0.0663	0.0605	0.0483	0.0422	0.0655	0.0489

[a] Reference 52. [b] Reference 53. [c] R_1 ($F > 5\sigma(F)$).

CHART 3. [a]

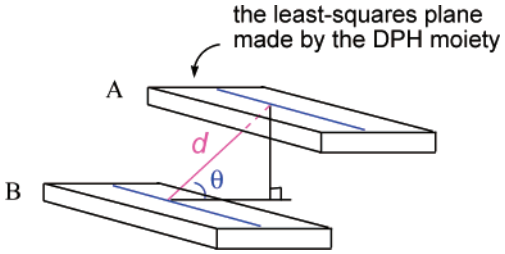

[a] *d* is the shortest intermolecular distance between triene carbons. Molecules A and B in each crystal are shown in Figure 4.

TABLE 5: Values of *d* and *θ* for Molecules A and B in the Crystals of 3−6 and 1/5

compd	*d* (Å)	*θ* (deg)
3	5.824	12.04
4	5.924	14.26
5	4.906	33.55
6	3.734	62.65
1/5	3.813	57.76

R band intensity for **3** and **4** relative to those for **1** and **2** can be understood in terms of stronger interactions in the π-stacked structures.

5.2. Fluorescence Properties. The weak $\pi-\pi$ interactions in the herringbone structures of **1** and **2** also account for their predominantly monomeric origin of emission. Although the difference in the strength of $\pi-\pi$ interaction in **1**−**4** is probably reflected in the absorption spectra as mentioned above, crystals **3** and **4** also exhibited mainly monomeric emission. This suggests that the interactions in **3** and **4** are still weak due to their largely offset structures.

Considering its offset stacking structure, the excimer emission from crystal **5** was rather unexpected, since the formation of excimer requires strong interactions between π-orbitals.

Crystals of **6** and **1/5** had similar, nearly face-to-face stacking structures. Strong $\pi-\pi$ interactions were expected in these cases, and as a result of this, they similarly exhibited largely red-shifted emission relative to those of the other compounds. Interestingly, however, the origin of the red-shifted emission was clearly different for **6** and **1/5**. The observation of excimer fluorescence from **6** indicates that the two (or more) molecules in the crystal strongly interact in the excited state, whereas in the ground state they experience a mutual repulsion. On the other hand, **1/5** exhibited the emission from the excited states of molecular aggregates in which molecules of **1** and **5** strongly interact already in the ground state. The strong intermolecular interaction between **1** and **5** may be correlated with the difference in the electron affinity (reduction potential) between these molecules. For fluorinated distyrylbenzenes, the electron affinity increases as the number of the fluorine atoms on the rings increases.[45] Analogously, we can expect that the most fluorinated **5** in this study has higher electron affinity than nonfluorinated **1**. If this is the case, then it may safely be said that the molecular aggregate in **1/5** is a CT complex in the solid state.

The present results can be compared with our previous observation for (*E*,*E*,*E*)-*p*-nitro-*p*′-alkoxy-substituted DPHs.[33] The crystal of the nitro-*n*-butoxy derivative had π-stacked structure with $d = 3.7$ Å and $\theta = 67°$, both of which are similar to the values in **6**. Different from the case of **6**, however, it exhibited pure monomeric emission. Again these indicate that, even if the molecular arrangements of the π-conjugated fluorophores are very similar in the crystals, the strength of orbital−

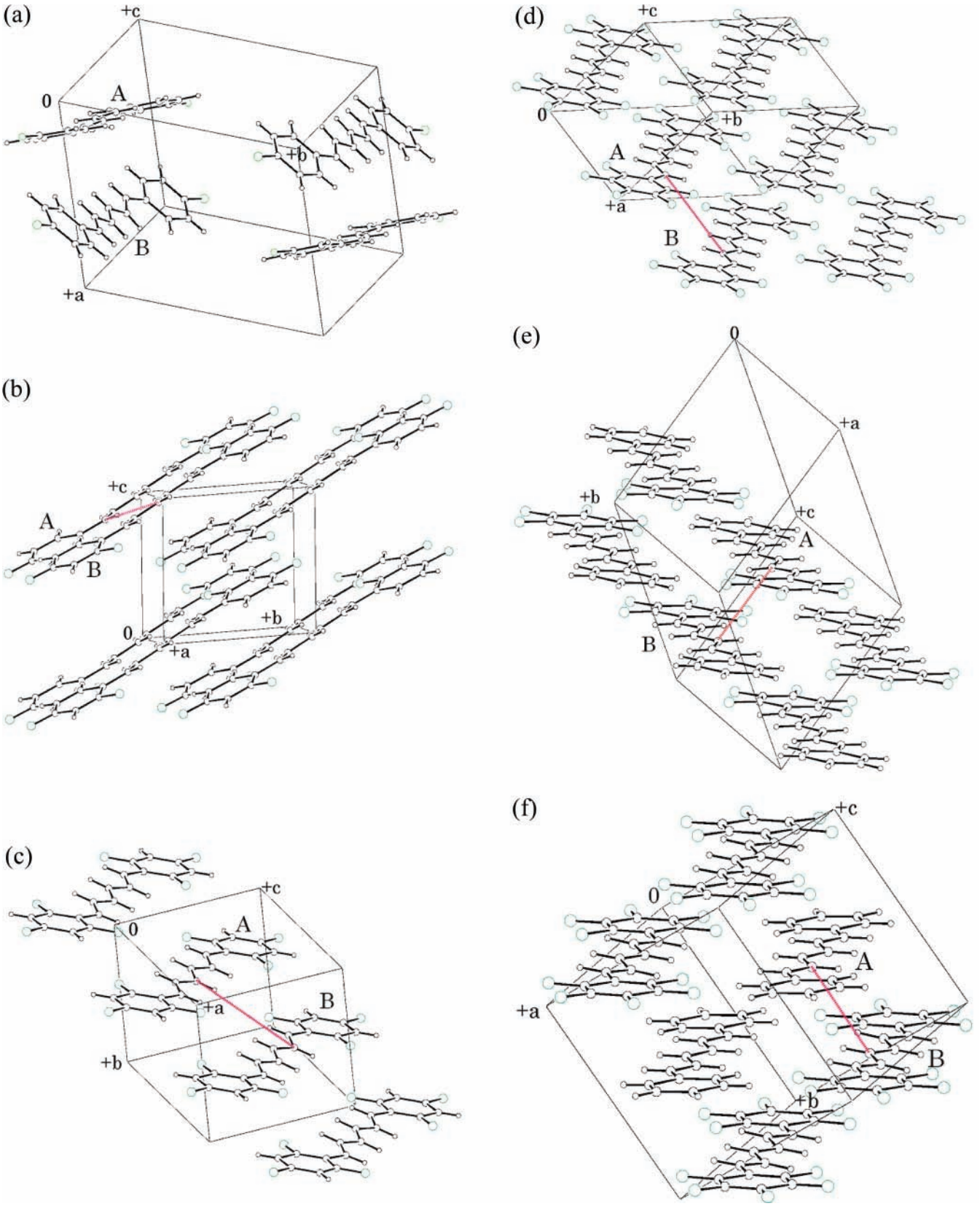

Figure 4. Crystal packing diagrams of (a) **2**, (b) **3**, (c) **4**, (d) **5**, (e) **6**, and (f) **1/5**.

orbital interaction between molecular π-planes in the ground and the excited states can be entirely different.

Conclusions

The solid-state absorption and fluorescence spectra of **1**−**6** and **1/5** were strongly dependent on the fluorine ring substituent. The spectral red shifts relative to those in solution would be mainly due to the planarization of the molecule in the solid state. The strong substituent dependence of the solid-state spectra arises from the difference in the strength of interaction between DPH π-planes in the crystals, depending on the packing pattern. The weak $\pi-\pi$ interactions in the herringbone structures (**1**, **2**)

or in the largely offset stacking structures (**3**−**5**) account for their predominantly monomeric origin of emission. Considering the offset stacking structure due to $C_6F_5\cdots C_6F_5$ interaction, the observation of the excimer fluorescence from **5** was rather unexpected. Crystals **6** and **1/5** had similar, nearly face-to-face stacking structures due to strongly attractive $C_6F_5\cdots C_6H_5$ interaction. The largely red-shifted emission from **6** and **1/5** results from strong $\pi-\pi$ interaction in these crystals. Despite the similarity in the molecular arrangement in the crystal, however, the fluorescence origin was clearly different for **6** and **1/5**. This can be ascribed to the difference in the strength of orbital−orbital interaction between molecular π-planes in the ground and excited states.

Acknowledgment. We thank Dr. M. Tamura (AIST) for the measurements of ^{19}F NMR spectra and Dr Y. Kawanishi (AIST) for the use of his fluorescence spectrometer.

Supporting Information Available: Crystallographic data for **2**−**6** and **1/5** in CIF format; preparation procedure for **14**; crystal and structure refinement data for **2**−**6** and **1/5**; absorption and fluorescence spectra of **1** and **2** in solution; fluorescence data of **6** in solution; ORTEP representations for the molecular structures of **1**−**6** and **1/5**; results of quantum chemical calculations; molecular planarity data for crystals **1**−**6** and **1/5**. This material is available free of charge via the Internet at http://pubs.acs.org.

References and Notes

(1) (a) Kraft, A.; Grimsdale, A. C.; Holmes, A. B. *Angew. Chem., Int. Ed.* **1998**, *37*, 402. (b) Ho, P. K. H.; Thomas, D. S.; Friend, R. H.; Tessler, N. *Science* **1999**, *285*, 233. (c) Friend, R. H.; Gymer, R. W.; Holmes, A. B.; Burroughes, J. H.; Marks, R. N.; Taliani, C.; Bradley, D. D. C.; Dos Santos, D. A.; Brédas, J. L.; Lögdlund, M.; Salaneck, W. R. *Nature* **1999**, *397*, 121. (d) Bernius, M. T.; Inbasekaran, M.; O'Brien, J.; Wu, W. *Adv. Mater.* **2000**, *12*, 1737.

(2) Heeger, A. J. *Solid State Commun.* **1998**, *107*, 673.

(3) Van Hutten, P. F.; Krasnikov, V. V.; Hadziioannou, G. *Acc. Chem. Res.* **1999**, *32*, 257.

(4) (a) Hide, F.; Díaz-García, M. A.; Schwartz, B. J.; Andersson, M. R.; Pei, Q.; Heeger, A. J. *Science* **1996**, *273*, 1833. (b) Tessler, N.; Denton, G. J.; Friend, R. H. *Nature* **1996**, *382*, 695.

(5) Pei, Q.; Yu, G.; Zhang, C.; Yang, Y.; Heeger, A. J. *Science* **1995**, *269*, 1086.

(6) Selected from recent studies: (a) Wolak, M. A.; Jang, B.-B.; Palilis, L. C.; Kafafi, Z. H. *J. Phys. Chem. B* **2004**, *108*, 5492. (b) Zhang, H.; Yang, B.; Zheng, Y.; Yang, G.; Ye, L.; Ma, Y.; Chen, X.; Cheng, G.; Liu, S. *J. Phys. Chem. B* **2004**, *108*, 9571. (c) Sakuda, E.; Tsuge, K.; Sasaki, Y.; Kitamura, N. *J. Phys. Chem. B* **2005**, *109*, 22326. (d) Tonzola, C. J.; Kulkarni, A. P.; Gifford, A. P.; Kaminsky, W.; Jenekhe, S. A. *Adv. Funct. Mater.* **2007**, *17*, 863.

(7) Oelkrug, D.; Tompert, A.; Gierschner, J.; Egelhaaf, H.-J.; Hanack, M.; Hohloch, M.; Steinhuber, E. *J. Phys. Chem. B* **1998**, *102*, 1902.

(8) (a) Xie, Z.; Yang, B.; Li, F.; Cheng, G.; Liu, L.; Yang, G.; Xu, H.; Ye, L.; Hanif, M.; Liu, S.; Ma, D.; Ma, Y. *J. Am. Chem. Soc.* **2005**, *127*, 14152. (b) Li, Y.; Li, F.; Zhang, H.; Xie, Z.; Xie, W.; Xu, H.; Li, B.; Shen, F.; Ye, L.; Hanif, M.; Ma, D.; Ma, Y. *Chem. Commun.* **2007**, 231.

(9) (a) Wu, C. C.; DeLong, M. C.; Vardeny, Z. V.; Ferraris, J. P. *Synth. Met.* **2003**, *137*, 939. (b) Bhongale, C. J.; Chang, C.-W.; Lee, C.-S.; Diau, E. W.-G.; Hsu, C.-S. *J. Phys. Chem. B* **2005**, *109*, 13472.

(10) (a) Chen, X.; Tseng, H.-E.; Liao, J.-L.; Chen, S.-A. *J. Phys. Chem. B* **2005**, *109*, 17496. (b) Hung, M.-C.; Liao, J.-L.; Chen, S.-A.; Chen, S.-H.; Su, A.-C. *J. Am. Chem. Soc.* **2005**, *127*, 14576. (c) Zhu, Y.; Gibbons, K. M.; Kulkarni, A. P.; Jenekhe, S. A. *Macromolecules* **2007**, *40*, 804.

(11) Qu, L.; Shi, G. *Chem. Commun.* **2004**, 2800.

(12) (a) de Halleux, V.; Calbert, J.-P.; Brocorens, P.; Cornil, J.; Declercq, J.-P.; Brédas, J.-L.; Geerts, Y. *Adv. Funct. Mater.* **2004**, *14*, 649. (b) Hayer, A.; de Halleux, V.; Köhler, A.; El-Garoughy, A.; Meijer, E. W.; Barberá, J.; Tant, J.; Levin, J.; Lehmann, M.; Gierschner, J.; Cornil, J.; Geerts, Y. H. *J. Phys. Chem. B* **2006**, *110*, 7653.

(13) Reichenbächer, K.; Süss, H. I.; Hulliger, J. *Chem. Soc. Rev.* **2005**, *34*, 22.

(14) Patrick, C. R.; Prosser, G. S. *Nature* **1960**, *187*, 1021.

(15) (a) Brock, C. P.; Naae, D. G.; Goodhand, N.; Hamor, T. A. *Acta Crystallogr.* **1978**, *B34*, 3691. (b) Naae, D. G. *Acta Crystallogr.* **1979**, *B35*, 2765.

(16) (a) Bartholomew, G. P.; Bazan, G. C.; Bu, X.; Lachicotte, R. J. *Chem. Mater.* **2000**, *12*, 1422. (b) Bartholomew, G. P.; Bu, X.; Bazan, G. C. *Chem. Mater.* **2000**, *12*, 2311. (c) Feast, W. J.; Lövenich, P. W.; Puschmann, H.; Taliani, C. *Chem. Commun.* **2001**, 505.

(17) (a) Ponzini, F.; Zagha, R.; Hardcastle, K.; Siegel, J. S. *Angew. Chem., Int. Ed.* **2000**, *39*, 2323. (b) Watt, S. W.; Dai, C.; Scott, A. J.; Burke, J. M.; Thomas, R. Ll.; Collings, J. C.; Viney, C.; Clegg, W.; Marder, T. B. *Angew. Chem., Int. Ed.* **2004**, *43*, 3061. (c) Smith, C. E.; Smith, P. S.; Thomas, R. Ll.; Robins, E. G.; Collings, J. C.; Dai, C.; Scott, A. J.; Borwick, S.; Batsanov, A. S.; Watt, S. W.; Clark, S. J.; Viney, C.; Howard, J. A. K.; Clegg, W.; Marder, T. B. *J. Mater. Chem.* **2004**, *14*, 413.

(18) (a) Bunz, U. H. F.; Enkelmann, V. *Chem.—Eur. J.* **1999**, *5*, 263. (b) Nishinaga, T.; Nodera, N.; Miyata, Y.; Komatsu, K. *J. Org. Chem.* **2002**, *67*, 6091.

(19) Sonoda, Y. *CRC Handbook of Organic Photochemistry and Photobiology*, 2nd ed.; Horspool, W., Lenci, F., Eds.; CRC Press: Boca Raton, FL, 2004; Chapter 73.

(20) Coates, G. W.; Dunn, A. R.; Henling, L. M.; Ziller, J. W.; Lobkovsky, E. B.; Grubbs, R. H. *J. Am. Chem. Soc.* **1998**, *120*, 3641.

(21) Topochemical photopolymerization of diacetylenes utilizing perfluorophenyl−phenyl interactions in the crystalline state has also been reported: (a) Coates, G. W.; Dunn, A. R.; Henling, L. M.; Dougherty, D. A.; Grubbs, R. H. *Angew. Chem., Int. Ed.* **1997**, *36*, 248. (b) Xu, R.; Gramlich, V.; Frauenrath, H. *J. Am. Chem. Soc.* **2006**, *128*, 5541.

(22) (a) Weck, M.; Dunn, A. R.; Matsumoto, K.; Coates, G. W.; Lobkovsky, E. B.; Grubbs, R. H. *Angew. Chem., Int. Ed.* **1999**, *38*, 2741. (b) Dai, C.; Nguyen, P.; Marder, T. B.; Scott, A. J.; Clegg, W.; Viney, C. *Chem. Commun.* **1999**, 2493. (c) Kishikawa, K.; Oda, K.; Aikyo, S.; Kohmoto, S. *Angew. Chem., Int. Ed.* **2007**, *46*, 764.

(23) Kilbinger, A. F. M.; Grubbs, R. H. *Angew. Chem., Int. Ed.* **2002**, *41*, 1563.

(24) Kim, T.-D.; Kang, J.-W.; Luo, J.; Jang, S.-H.; Ka, J.-W.; Tucker, N.; Benedict, J. B.; Dalton, L. R.; Gray, T.; Overney, R. M.; Park, D. H.; Herman, W. N.; Jen, A. K.-Y. *J. Am. Chem. Soc.* **2007**, *129*, 488.

(25) Shu, L.; Mu, Z.; Fuchs, H.; Chi, L.; Mayor, M. *Chem. Commun.* **2006**, 1862.

(26) (a) Cozzi, F.; Ponzini, F.; Annunziata, R.; Cinquini, M.; Siegel, J. S. *Angew. Chem., Int. Ed.* **1995**, *34*, 1019. (b) Cozzi, F.; Siegel, J. S. *Pure Appl. Chem.* **1995**, *67*, 683.

(27) (a) Adams, H.; Blanco, J.-L. J.; Chessari, G.; Hunter, C. A.; Low, C. M. R.; Sanderson, J. M.; Vinter, J. G. *Chem.—Eur. J.* **2001**, *7*, 3494. (b) Gung, B. W.; Patel, M.; Xue, X. *J. Org. Chem.* **2005**, *70*, 10532. (c) Gung, B. W.; Xue, X.; Zou, Y. *J. Org. Chem.* **2007**, *72*, 2469.

(28) (a) Tsuzuki, S.; Uchimaru, T.; Mikami, M. *J. Phys. Chem. A* **2006**, *110*, 2027. (b) Ringer, A. L.; Sinnokrot, M. O.; Lively, R. P.; Sherrill, C. D. *Chem.—Eur. J.* **2006**, *12*, 3821. (c) Gung, B. W.; Amicangelo, J. C. *J. Org. Chem.* **2006**, *71*, 9261.

(29) Frontera, A.; Quiñonero, D.; Costa, A.; Ballester, P.; Deyà, P. M. *New J. Chem.* **2007**, *31*, 556.

(30) The optical spectra for the thin films of fluorinated oligo(phenylenevinylene)s have been reported: Strehmel, B.; Sarker, A. M.; Malpert, J. H.; Strehmel, V.; Seifert, H.; Neckers, D. C. *J. Am. Chem. Soc.* **1999**, *121*, 1226.

(31) Allen, M. T.; Whitten, D. G. *Chem. Rev.* **1989**, *89*, 1691.

(32) Sonoda, Y.; Kawanishi, Y.; Ikeda, T.; Goto, M.; Hayashi, S.; Yoshida, Y.; Tanigaki, N.; Yase, K. *J. Phys. Chem. B* **2003**, *107*, 3376.

(33) Sonoda, Y.; Goto, M.; Tsuzuki, S.; Tamaoki, N. *J. Phys. Chem. A* **2006**, *110*, 13379.

(34) McDonald, R. N.; Campbell, T. W. *J. Org. Chem.* **1959**, *24*, 1969.

(35) (a) Alford, P. C.; Palmer, T. F. *Chem. Phys. Lett.* **1982**, *86*, 248. (b) Alford, P. C.; Palmer, T. F. *J. Chem. Soc., Faraday Trans. 2* **1983**, *79*, 433. (c) Alford, P. C.; Palmer, T. F. *Chem. Phys. Lett.* **1986**, *127*, 19.

(36) Melhuish, W. H. *J. Phys. Chem.* **1961**, *65*, 229.

(37) Birks, J. B.; Kazzaz, A. A.; King, T. A. *Proc. R. Soc., London* **1966**, *A291*, 556.

(38) *SMART*, version 5.625; Bruker AXS: Madison, WI, 2001. *SAINT-PLUS*, version 6.22; Bruker AXS: Madison, WI, 2001. Sheldrick, G. M. *SADABS, Program for scaling and correction of area, detector data*; University of Göttingen: Germany, 1998, 2001.

(39) Altomare, A.; Cascarano, G.; Giacovazzo, C.; Guagliardi, A.; Brula, M. C.; Polidori, G.; Camalli, M. *J. Appl. Crystallogr.* **1994**, *27*, 435.

(40) Sheldrick, G. M. *SHELXTL*, version 6.12; Bruker AXS: Madison, WI, 2000.

(41) Frisch, M. J.; Trucks, G. W.; Schlegel, H. B.; Scuseria, G. E.; Robb, M. A.; Cheeseman, J. R.; Montgomery, J. A., Jr.; Vreven, T.; Kudin, K. N.; Burant, J. C.; Millam, J. M.; Iyengar, S. S.; Tomasi, J.; Barone, V.; Mennucci, B.; Cossi, M.; Scalmani, G.; Rega, N.; Petersson, G. A.; Nakatsuji, H.; Hada, M.; Ehara, M.; Toyota, K.; Fukuda, R.; Hasegawa, J.;

Ishida, M.; Nakajima, T.; Honda, Y.; Kitao, O.; Nakai, H.; Klene, M.; Li, X.; Knox, J. E.; Hratchian, H. P.; Cross, J. B.; Bakken, V.; Adamo, C.; Jaramillo, J.; Gomperts, R.; Stratmann, R. E.; Yazyev, O.; Austin, A. J.; Cammi, R.; Pomelli, C.; Ochterski, J. W.; Ayala, P. Y.; Morokuma, K.; Voth, G. A.; Salvador, P.; Dannenberg, J. J.; Zakrzewski, V. G.; Dapprich, S.; Daniels, A. D.; Strain, M. C.; Farkas, O.; Malick, D. K.; Rabuck, A. D.; Raghavachari, K.; Foresman, J. B.; Ortiz, J. V.; Cui, Q.; Baboul, A. G.; Clifford, S.; Cioslowski, J.; Stefanov, B. B.; Liu, G.; Liashenko, A.; Piskorz, P.; Komaromi, I.; Martin, R. L.; Fox, D. J.; Keith, T.; Al-Laham, M. A.; Peng, C. Y.; Nanayakkara, A.; Challacombe, M.; Gill, P. M. W.; Johnson, B.; Chen, W.; Wong, M. W.; Gonzalez, C.; Pople, J. A. *Gaussian 03*, revision C.02; Gaussian, Inc.: Wallingford, CT, 2004.

(42) Foresman, J. B.; Head-Gordon, M.; Pople, J. A.; Frisch, M. J. *J. Phys. Chem.* **1992**, *96*, 135.

(43) (a) Lee, C.; Yang, W.; Parr, R. G. *Phys. Rev. B* **1988**, *37*, 785. (b) Becke, A. D. *J. Chem. Phys.* **1993**, *98*, 5648. (c) Stratmann, R. E.; Scuseria, G. E.; Frisch, M. J. *J. Chem. Phys.* **1998**, *109*, 8218.

(44) Cehelnik, E. D.; Cundall, R. B.; Lockwood, J. R.; Palmer, T. F. *J. Phys. Chem.* **1975**, *79*, 1369.

(45) Renak, M. L.; Bartholomew, G. P.; Wang, S.; Ricatto, P. J.; Lachicotte, R. J.; Bazan, G. C. *J. Am. Chem. Soc.* **1999**, *121*, 7787.

(46) (a) Lin-Vien, D.; Colthup, N. B.; Fateley, W. G.; Grasselli, J. G. *The Handbook of Infrared and Raman Characteristic Frequencies of Organic Molecules*; Academic Press: San Diego, CA, 1991. (b) Kohler, B. E. *Chem. Rev.* **1993**, *93*, 41.

(47) Klessinger, M.; Michl, J. *Excited States and Photochemistry of Organic Molecules*; VCH Publishers, Inc.: New York, 1995; Chapter 1.

(48) The obtained ϕ_f values for **1** and **2** were smaller and τ_s values were shorter than the reported values.[35] Considering that our ϕ_f and τ_s values were those measured for air-saturated solution whereas the reported ones are obtained for degassed samples, the discrepancies are probably due to the fluorescence quenching by molecular oxygen in air.[36] It should be noted that k_f for **1** and **2** calculated from our data agreed well with those reported.

(49) The *Z*−*E* photoisomerization of **1**−**5** was inefficient in MCH. The isomerization of **6** was checked by HPLC. For the photoisomerization of symmetrically and unsymmetrically substituted DPHs in solution, see: (a) Sonoda, Y.; Suzuki, Y. *Chem. Lett.* **1996**, 659. (b) Sonoda, Y.; Morii, H.; Sakuragi, M.; Suzuki, Y. *Chem. Lett.* **1998**, 349. (c) Sonoda, Y.; Kawanishi, Y.; Sakuragi, M. *Chem. Lett.* **1999**, 587. (d) Sonoda, Y.; Kawanishi, Y. *Chem. Lett.* **2003**, *32*, 978.

(50) Jenekhe, S. A.; Osaheni, J. A. *Science* **1994**, *265*, 765.

(51) Mikroyannidis, J. A.; Fenenko, L.; Adachi, C. *J. Phys. Chem. B* **2006**, *110*, 20317.

(52) Hall, T.; Bachrach, S. M.; Spangler, C. W.; Sapochak, L. S.; Lin, C. T.; Guan, H. W.; Rogers, R. D. *Acta Crystallogr.* **1989**, *C45*, 1541.

(53) Sonoda, Y.; Suzuki, Y. *J. Chem. Soc., Perkin Trans. 2* **1996**, 401.

(54) It is noteworthy that the crystal of the chloro analogue of **3** has herringbone structure with the shortest intermolecular Cl···Cl distance of 3.514 Å.[55] The difference in crystal packing may be ascribed to the weaker F···F interaction than Cl···Cl interaction, resulting from less polarizable nature of the fluorine atoms.[56]

(55) Sonoda, Y.; Kawanishi, Y.; Goto, M. *Acta Crystallogr.* **2003**, *C59*, o311.

(56) Thalladi, V. R.; Weiss, H.-C.; Boese, R.; Nangia, A.; Desiraju, G. R. *Acta Crystallogr.* **1999**, *B55*, 1005.

(57) Liu, J.; Murray, E. M.; Young, V. G., Jr. *Chem. Commun.* **2003**, 1904.

(58) The similarities for the structures of C_6F_5—C≡C—C_6H_5 vs cocrystal C_6F_5—C≡C—C_6F_5/C_6H_5—C≡C—C_6H_5 and for C_6F_5—C≡C—C≡C—C_6H_5 vs cocrystal C_6F_5—C≡C—C≡C—C_6F_5/C_6H_5—C≡C—C≡C—C_6H_5 were previously noted in refs 17c and 21a, respectively.

(59) Tsuzuki, S. Unpublished work.